*International Journal of Microwave and Wireless Technologies*, 2011, 3(4), 485–491. 
doi:10.1017/S1759078711000493

INDUSTRIAL AND ENGINEERING PAPER

# Design of a compact quarter wave coaxial cavity resonator for plasma ignition applications

FRANZ A. PERTL[1], MARY ANN CLARKE[2] AND JAMES E. SMITH[1]

*Atmospheric and higher pressure RF and microwave plasma sources have numerous applications including material processing and spectroscopy. More recently, advantages in using such discharges for combustion ignition are being investigated. A particularly simple and compact microwave discharge generating device is the quarter wave coaxial cavity resonator (QWCCR). This paper presents a new, compacted design of such a device. A simple approximate analysis of the quality factor, Q, which is a measure of the resonant electromagnetic potential step-up capability is given, and compared to experimentally measured quality factors showing reasonable agreement. Analytic results indicate that the foreshortened folded cavity quality factors are comparable to tapered coaxial cavity designs.*

**Keywords:** microwave plasma ignition, microwave cavity, quarter wave coaxial cavity resonator

Received 13 July 2010; Revised 28 February 2011; first published online 12 May 2011

## I. INTRODUCTION

One particularly simple device for generating an atmospheric or higher pressure RF or microwave plasma is the quarter wave coaxial cavity resonator (QWCCR). As an alternative to a traditional sparkplug used for initiating combustion, such a device has been studied by researchers at the West Virginia University's Mechanical and Aerospace Engineering Department for a number of years [1–10]. A recent publication [8] shows that the minimum required ignition energy of the QWCCR is comparable to that of a sparkplug. Numerical simulations and experimental investigations of various cavity geometries have been performed in [6, 11]. An analytic approach relating cavity parameters to the developed electric field strengths that lead to gas breakdown and plasma formation have been published in [12].

The losses in the cavity, in particular the aperture radiation losses, can substantially lower the resonant step-up potential of the device as characterized by the quality factor, $Q$, of the cavity. This is especially true when the aperture size is not negligible with respect to the operating wavelength $\lambda$. This has lead to empirical geometries which reduce the aperture through tapering of the cavity, an example of which is shown in Fig. 1. Such tapered and straight cavity designs are, at a minimum, approximately a quarter wavelength ($\lambda/4$) in physical size. Naturally, larger odd multiples of $\lambda/4$ could also be used to make longer devices. Using the shortest $\lambda/4$ size, at a frequency of 2.45 GHz the approximate cavity length is 3 cm. To make the physical size of these resonators practical, and comparable to sparkplugs, such GHz range frequency have been used, but this is not necessarily desirable from a cavity wall conduction loss point of view, since conduction losses increase with operating frequency.

The current document makes use of the previous work presented in [12] to approximately characterize more compact, shorter, nested QWCCR designs with a smaller aperture-to-wavelength ratio. Additionally, these designs are of practical length even at lower frequencies; and a reduction in cavity wall surface resistance, $R_s$, is beneficial for maintaining a high $Q$ factor. Note reduction of operating frequency can also be accomplished through reactive loading of the cavity, or by filling the interior with a dielectric. However, these approaches add additional $Q$ lowering losses, especially if the loss tangent of the material and its dielectric constant are relatively large.

## II. SHORTENED CONCENTRICALLY NESTED DESIGN

The folded design consists of concentrically connected segments of coaxial transmission line. The radial dimensions have been chosen to maintain a uniform transmission line impedance from the RF input end of the cavity to the discharge end. While it may be practical, as mentioned above, to fill the entire interior of the igniter with a dielectric to

[1]Department of Mechanical and Aerospace Engineering, West Virginia University, Morgantown, WV 26506, USA. Phone: + 1 304 293 3256.
[2]Department of Mathematics, West Virginia University, Morgantown, WV 26506, USA.
**Corresponding author:**
F. A. Pertl
Email: franz.pertl@mail.wvu.edu

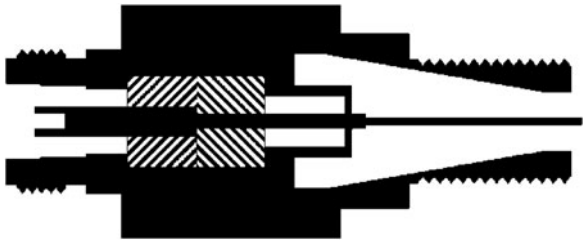

**Fig. 1.** Cross sectional view of small aperture 2.45 GHz tapered cavity design.

**Fig. 2.** 3D view of folded QWCCR design concept.

reduce its electrical length, $z$, the disadvantage is again the additional dielectric loss incurred. For this reason, only very short dielectric washers have been employed in the folded design to seal the device from the combustion chamber. This also avoids potential thermal expansion rate differences between metal and dielectric which in the case of ceramics may lead to cracking. A 3D view of a potential design showing the concentric coaxial segments is given in Fig. 2.

The dimension of this design target is 433 MHz. The 2D view in Fig. 3 shows more clearly the manner in which the transmission line segments are connected. RF feeds in via the N-type connector on the left, couples into the cavity with a loop structure, and then travels to the right in the outer most space until it is reflected by the short circuit on the right-hand side into the volume of the structure that formed the center conductor of the outer most section. The wave then switches direction and travels to the left until the end of this inner volume, where the previous process is repeated, until the open end of the cavity is reached. The entire path is electrically one-quarter wavelength long. As mentioned previously, higher odd multiples of quarter wavelength could also be used. The portions of the inner section contain low-loss dielectric disks to seal the resonator from the combustion and to maintain impedance as the geometry changes. An approximately equivalent unfolded structure is shown in Fig. 4. Note that the shorting plates are now

**Fig. 4.** 2D view of unfolded equivalent structure.

sandwiched between dielectric regions for an overall length that is twice the dielectric washer length compared to Fig. 3. The transmission line sections' radii were chosen to have an outer to inner radius ratio, $b/a$, approximately equal to 1.88. This was done to exploit conveniently available tube sizes, but other ratios could be used. Explicit values for the dimension of this design are given in Table 1. With a free-space intrinsic impedance of $\eta = \sqrt{\mu_o/\varepsilon_o} = 377\,\Omega$, this resulting transmission line impedance, $Z_o = \eta/2\pi \ln(b/a)$ equals 38 Ω, a reasonable value considering the theoretical optimums for the lowest loss is 77 Ω, and for highest field handling capabilities is 30 Ω [13].

## III. ANALYSIS OF NESTED DESIGN

Ultimately, whether plasma is formed or not, depends on the breakdown strength of the gas mixture and the field strength at the discharge electrode tip. The developed electric field, $E_{a\text{-}tip}$, at the tip of the quarter wave cavity can be related to the power, $P$, fed into the cavity, its quality factor, and the tip geometry [12]. Assuming an unsharpened rounded tip with a spherical radius of curvature equal to the electrode radius, $a_{tip}$, at a potential, $V_o$, the tip field can be approximated by

$$E_{a-tip} = \frac{V_o}{2\pi a_{tip}}. \tag{1}$$

At resonance, the tip potential, $V_o$, is proportional to the time average energy, $U$, stored in the cavity, volume that is related to the quality factor, $Q$, is given by

$$V_o^2 \propto U = \frac{QP}{\omega}, \tag{2}$$

where $\omega$ is the angular resonant frequency. The time average energy stored in the cavity can be found from

$$U = \frac{1}{4}\int_{vol} \varepsilon|\mathbf{E}|^2 + \mu|\mathbf{H}|^2 dv = \frac{QP}{\omega}. \tag{3}$$

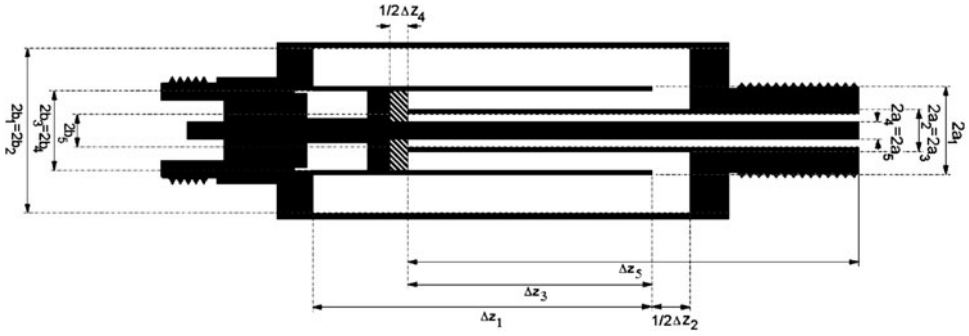


**Fig. 3.** 2D view of folded QWCCR design, see Table 1 for dimension values.

https://doi.org/10.1017/S1759078711000493 Published online by Cambridge University Press

This is the integration of the energy density of the electric field **E** and the magnetic field **H**, over the volume of the cavity. Note that at resonance the magnetic and electric stored time average energies are equal. The energy stored per unit length is not directly dependent of the actual radii of the coaxial line section, but is a function of the line's characteristic impedance, i.e. the radius ratio. This means that the equations for stored energy in a quarter wave resonant section do not change even if parts of the line are reduced in diameter, provided the characteristic impedance is preserved. The equations for the tip electric field magnitude, (4), and the equation for the cavity stored energy as given in [12] are still applicable:

$$E_a = \frac{2}{\pi a_{tip}}\sqrt{\frac{\eta Q P}{\ln(b/a)}} \tag{4}$$

and

$$U = \frac{\mu I_o^2 \ln(b/a)\lambda/4}{8\pi}. \tag{5}$$

Using the relation between wavelength, $\lambda$, frequency, $f$, and propagation velocity, $(\mu \cdot \varepsilon)^{-1/2}$, these equations can also be expressed in terms of the characteristic impedance of the line, $Z_o$, by

$$E_a = \frac{\eta}{a_{tip}}\sqrt{\frac{2QP}{\pi^3 Z_o}} \tag{6}$$

and

$$U = \frac{I_o^2 Z_o}{16 f}. \tag{7}$$

This shows that stored energy increases with line impedance, $Z_o$, and decreases with frequency, $f$. What remains is to examine the losses of the transmission line sections. This can be done by assuming the field fringing at the internal corners of the line junction points are negligible, and that the fields of the resonance are approximately transverse electromagnetic mode (TEM) standing quarter wave sinusoids such that

$$\mathbf{H} = \frac{I_o}{2\pi r}\cos(\beta z)\hat{\mathbf{a}}_\phi \tag{8}$$

and

$$\mathbf{E} = \frac{\eta I_o}{2\pi r}\sin(\beta z)\hat{\mathbf{a}}_r \tag{9}$$

where $\beta = 2\pi/\lambda$ and $I_o$ is some assumed amplitude. For a cylindrical conductor surface, with surface resistance $R_s$, and radius $r_o$, the time average power dissipated is given by the surface integral

$$\begin{aligned} P_{cyl} &= \tfrac{R_s}{2}\int_A |\mathbf{H}_{//}|^2 dA, \\ P_{cyl} &= \tfrac{I_o^2 R_s}{4\pi\beta r_o}\int_{\theta_{z1}}^{\theta_{z2}} \cos^2(\theta_z)\, d\theta_z \end{aligned} \tag{10}$$

where dimensions along the line have been recast in terms of electrical angles so that $\beta \cdot dz = d\theta_z$. Considering an area interpretation of the integral over $\cos^2(\theta)$, it can be seen that losses per unit length decrease as the open end of the cavity is approached. This suggests that using large radii toward the short-circuited end of the resonant line is more important in reducing losses than using them toward the open-circuited end. If constant power dissipation per unit length is desired, the radii could vary as $r_o \cos^2(\theta)$ resulting in a tapered shape shown in Fig. 5. The sidewall surface loss of (10) would then reduce to

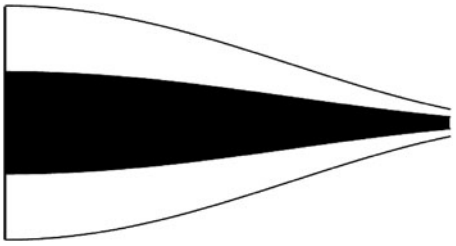

**Fig. 5.** $\cos^2$ tapered geometry for constant loss per unit length.

$$P_{\cos^2} = \frac{I_o^2 R_s}{4\pi\beta r_o}\Delta\theta_z. \tag{11}$$

Through a similar area integration the ohmic power losses for a circular annulus with inner and outer radius $a'$ and $b$, respectively, at a distance $z$ along the line is determined as

$$P_{anu} = \frac{I_o^2 R_s}{4\pi}\ln(b/a')\cos^2(\theta_z). \tag{12}$$

Placing annuli close to the short-circuited end of the transmission line, where the magnetic fields are higher, will result in larger losses. The power dissipated by the standing wave in a low-loss dielectric filling, with effective conductivity, $\sigma_e = \omega\varepsilon\tan(\delta)$, in the coaxial line with inner radius, $a$, and outer radius, $b$, extending between distances $z_1$ and $z_2$ along the line is

$$\begin{aligned} P_{\sigma_e} &= \tfrac{\sigma_e}{2}\int_{Vol}|E|^2 dv, \\ P_{\sigma_e} &= \tfrac{1}{2} I_o^2 Z_o \tan(\delta)\int_{\theta_{z1}}^{\theta_{z2}} \sin^2(\theta_z) d\theta_z \end{aligned} \tag{13}$$

for the sinusoidal resonant field distribution. Considering the integral over $\sin^2(\theta)$ in (13), the closer a dielectric filling is placed to the open end of the resonator, the higher the losses will be. The quality factors, $Q$, of the resonator can now be estimated as

$$Q = \left(\sum_i \frac{P_i}{\omega U}\right)^{-1}. \tag{14}$$

Prior to analyzing any design, the section lengths of the resonator have to be converted to electrical degrees so the integrals can be evaluated. The dielectric constant of the transition regions will affect the angular electrical line length. The relative dielectric constant required to maintain the same line impedance when the conductor radius ratio changes from

https://doi.org/10.1017/S1759078711000493 Published online by Cambridge University Press

**Table 1.** Dimension and properties of coaxial line sections.

| Coax | $c1$ | $c2$ | $c3$ | $c4$ | $c5$ |
|---|---|---|---|---|---|
| $b$ (cm) | 1.19 | 1.19 | 0.57 | 0.57 | 0.24 |
| $a$ (cm) | 0.64 | 0.30 | 0.30 | 0.13 | 0.13 |
| $\epsilon_r$ | 1 | 1 | 1 | 5.8 | 1 |
| tan($\delta$) | 0 | 0 | 0 | .005 | 0 |
| $Z_o$ ($\Omega$) | 38 | 82 | 38 | 38 | 37 |
| $\Delta z$ (cm) | 4.90 | 1.11 | 3.53 | 0.53 | 6.51 |
| $\Delta\theta_z$ (°) | 25.5 | 5.8 | 18.3 | 6.7 | 33.8 |
| $Q_i$ | 1700 | 5400 | 1900 | 1900 | 2200 |
| $\Delta$ ($zQ_i$ (cm$^{-1}$) | 8400 | 5800 | 6600 | 1000 | 14 500 |

**Table 2.** Dimensions and location of annuli.

| Annulus | $a0$ | $a1$ | $a2$ |
|---|---|---|---|
| $b$ (cm) | 1.19 | 1.19 | 0.57 |
| $a'$ (cm) | 0.64 | 0.30 | 0.13 |
| $z$ (cm) | 0.00 | 5.46 | 9.80 |
| $\theta_z$ (°) | 0 | 28.4 | 53.0 |
| $Q_i$ | 30 300 | 18 000 | 34 700 |

$b_o/a_o$ to $b_1/a_1$ is given by

$$\varepsilon_r = \left[\frac{\ln(b_1/a_1)}{\ln(b_o/a_o)}\right]^2. \tag{15}$$

For an initial test case, the structure shown in Fig. 4 was assembled out of commercially available brass tubing sizes targeting a resonance frequency of 433 MHz (69.3 cm wavelength) with dimensions as given in Tables 1 and 2. The value 0.0104 $\Omega$ was used as the surface resistance, $R_s$, of brass at 433 MHz. Note that the impedance matching dielectric at the first junction, which should have had a relative dielectric constant of 4.7, was omitted. Provided the length of the mismatch is short with respect to wavelength, no serious reflections will occur, and instead the junction steps will appear as small shunt capacitances. The magnitude of these capacitances can be estimated by the method outlined in chapter 6 of [14] and their combination is on the order of 0.2 pF which is located in a region of relatively low electric field magnitudes. For the purpose of this analysis, this shunt capacitance will be ignored (Fig. 6).

The calculated combined unloaded quality factor is 414. This is about 2.5 times greater than if the resonator had been made out of the smallest diameter section, $c5$, for the entire length, but naturally lower than if the larger diameters of section, $c1$, had been used throughout. It is apparent from the calculated $Q_i$, that the annuli losses are insignificant.

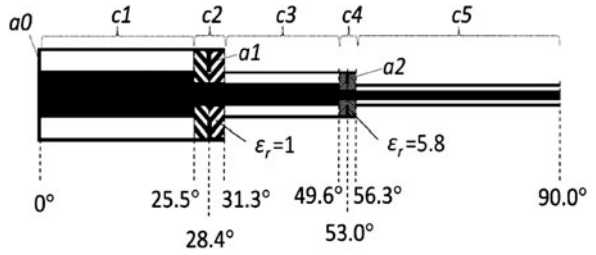


**Fig. 6.** Electrical angular lengths along unfolded equivalent structure.

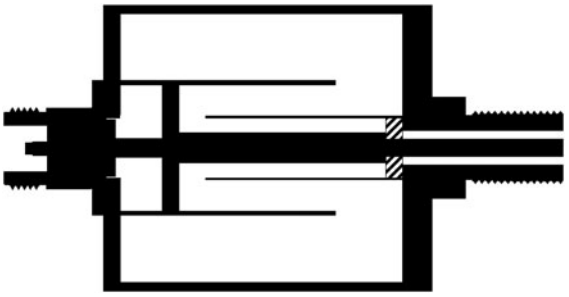

**Fig. 7.** 2D view of large radii folded QWCCR design.

However, the dielectric losses should not be discounted, despite the fact that the dielectric is set back from the maximum electric fields by 33.8°. Also of note is the fact that despite having the largest radii, the cylinders of the $c1$ section contribute the largest losses as it experiences the strongest magnetic fields.

As a figure of merit, that can be used to compare the transmission line sections, $\Delta zQ_i$ was also computed. This metric highlights the dielectric losses. Had the section not been kept short, the overall quality factor of the cavity would be drastically lowered. Improvements in the resonator's $Q$ can therefore be achieved by further increasing these radii. For the analysis to hold, the radii cannot be increased beyond the point where higher order modes start to appear in the cavity. This indicates that an upper limit should be set as $2\pi(b+a) < \lambda/2$ [15]. A compact cavity with larger radii, and assembled as shown in Fig. 7, was designed with dimensions given in Tables 3 and 4. The calculated, combined unloaded quality factor for this second design is 834, twice the small radii design quality factor. Note that an additional reduction in radii in going from $c5$ to $c7$ was included without a reversal in direction, and without accounting for the annuli losses in the reduction as the losses on the annuli are very low, i.e. their $Q$'s are very high.

As a comparison and using the same TEM assumptions, the quality factor of a $\cos^2(\theta)$ tapered, unfolded cavity of quarter wavelength using air as a dielectric was derived using: (7) for the energy stored, (11) for the tapered side conductors, and (12) for the base conductor annulus at the shorting end. The result without accounting for the dielectric is given by

$$Q_{\cos^2} = \left[\frac{\lambda R_s}{2\pi^2 Z_o}\left(\frac{1}{a}+\frac{1}{b}\right)+\frac{4R_s}{\pi\eta}\right]^{-1}. \tag{16}$$

The dielectric losses increase dramatically toward the open-circuited end of the cavity in such a tapered design since the $\sin^2(\theta)$ term under the integral in (13) is turned into a $\tan^2(\theta)$ term by the tapering:

$$\begin{aligned} P_{\sigma_c} &= \frac{\omega\varepsilon\eta^2 I_o^2}{4\pi}\int_{z1}^{z2}\int_a^b \frac{\sin^2(\beta z)}{r\cos^2(\beta z)}\,dr\,dz, \\ P_{\sigma_c} &= \frac{1}{2}I_o^2 Z_o \tan(\delta)\int_{\theta_{z1}}^{\theta_{z2}} \tan^2(\theta_z)\,d\theta_z. \end{aligned} \tag{17}$$

In an actual implementation, the length would be slightly shorter than $\lambda/4$, to allow an aperture that would have capacitance. Nevertheless, filling the entire cavity would create excessive losses. Since the previous two example cavities

https://doi.org/10.1017/S1759078711000493 Published online by Cambridge University Press

**Table 3.** Dimension and properties of coaxial line sections.

| Coax | *c*1 | *c*2 | *c*3 | *c*4 | *c*5 | *c*6 | *c*7 |
|---|---|---|---|---|---|---|---|
| $b$ (cm) | 2.53 | 2.53 | 1.19 | 1.19 | 0.56 | 0.56 | 0.28 |
| $a$ (cm) | 1.27 | 0.60 | 0.60 | 0.28 | 0.28 | 0.16 | 0.16 |
| $\epsilon_r$ | 1 | 1 | 1 | 1 | 1 | 5.8 | 1 |
| $\tan(\delta)$ | 0 | 0 | 0 | 0 | 0 | .005 | 0 |
| $Z_o$ ($\Omega$) | 42 | 88 | 41 | 87 | 42 | 31 | 34 |
| $\Delta z$ (cm) | 4.08 | 2.54 | 2.46 | 1.02 | 3.41 | 0.32 | 3.07 |
| $\Delta\theta_z(^\circ)$ | 21.2 | 13.2 | 12.8 | 5.3 | 17.7 | 4.0 | 15.9 |
| $Q_i$ | 5000 | 5600 | 6500 | 38 300 | 5400 | 3800 | 30 200 |
| $\Delta z Q_i$ ($\text{cm}^{-1}$) | 20 600 | 14 200 | 16 000 | 38 900 | 18 300 | 1300 | 92 700 |

**Table 4.** Dimensions and location of annuli.

| Annulus | *a*0 | *a*1 | *a*2 |
|---|---|---|---|
| $b$ (cm) | 2.53 | 2.53 | 1.19 |
| $a'$ (cm) | 1.27 | 0.60 | 0.28 |
| $z$ (cm) | 0.00 | 5.35 | 9.58 |
| $\theta_z$ ($^\circ$) | 0 | 27.8 | 49.8 |
| $Q_i$ | 33 600 | 20 500 | 12 300 |

were mostly hollow, the tapered cavity will be assumed to be made of brass with an air dielectric throughout. The resulting quality factors of the tapered design using the same radii at the shorted base as the two sectioned cavities are: 418 for the initial and 927 for the enlarged radii, respectively. These values are quite similar to the values calculated for the discretely sectioned designs; depending on how well the step tapered sections fit the $\cos^2(\theta)$ distribution, a first cut estimate of a sectioned design could be obtained using the tapered results. One could also construct such a tapered cavity by approximating the $\cos^2(\theta)$ taper with a straight line, thereby making a conical similar to Fig. 1.

**Fig. 8.** Large radii cavity at various stages of implementation.

## IV. SOME DESIGN IMPLEMENTATIONS

To check how valid the approximate analysis is, both designs were implemented with available brass tubing. The larger radii cavity is shown below in Fig. 8, at various stages of implementation.

Measurement of the quality factor and the degree of coupling on a HP8753D network analyzer resulted in an unloaded $Q$ of 340 at a resonance frequency of 425.75 MHz for the small radii geometry. The larger radii geometry resulted in an unloaded $Q$ of 760 with a resonance frequency of 439.87 MHz. The two assembled implementations are shown in Figs 9 and 10, respectively. A conical brass resonator had

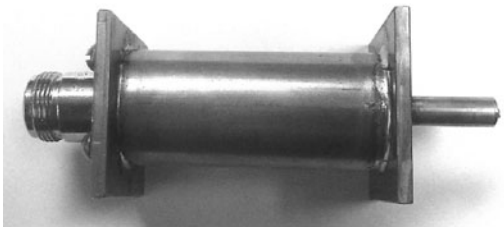

**Fig. 9.** Completed initial test case cavity.

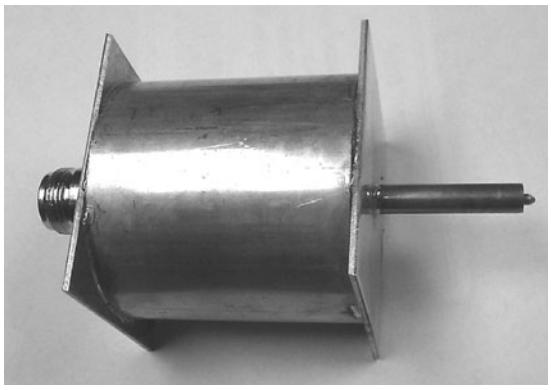

**Fig. 10.** Completed second test case cavity.

https://doi.org/10.1017/S1759078711000493 Published online by Cambridge University Press

been constructed some time ago with a base radius of 1.5″ and a $b/a$ ratio of 6 for an approximate line impedance of 108 Ω. Its resonance frequency had been measured at 960 MHz with an unloaded $Q$ of 1800 [16]. Calculations using the $\cos^2(\theta)$ taper results would predict a quality factor of 2100, with a 17% difference from the conical measured result. For the folded cavities constructed, the frequencies of the implementations of the first and second cavity differ from the design frequencies by 1.7 and 1.6%, respectively. As is generally the case, the measured quality factors were both lower than the theoretically calculated values. The respective differences for the small and large radii cavities were 18 and 9%. Note that disturbance of the electromagnetic fields at the base of the cavity due to the coupling structure have been ignored in the analysis. There is also potential for error due to conductivity differences, surface imperfections, solder joints, and uncertainty in the dielectric parameters.

## V. CONCLUSION

The feasibility of shortening the QWCCR by step tapering, and then concentrically nesting cylindrical structure inside of itself has been demonstrated. This allows more compact implementations of QWCCR and operation at lower frequencies where longer designs may be physically undesirable. When considering cavities designs that use odd multiples of $\lambda/4$ larger than one, the quality factor can be enhanced by making the high magnetic field sections along the cavity length have large radii.

An approximate analysis procedure to estimate the performance of such nested and tapered designs has been outlined. Despite considerable simplifications, the presented method can be used to estimate quality factors of the tapered and nested designs. More accurate results can be obtained with exact field distributions including fringing and capacitive loading at the step discontinuities. The approximate results suffice to allow the estimation of the approximate power requirements, $P$, in order to achieve breakdown and plasma formation for a given tip radius via (6). The folded cavity design performance is comparable with the performance of tapered design.

## REFERENCES

[1] Nash, M.A.: The coaxial cavity resonator and R.F. power processing, Master Thesis, West Virginia University, Morgantown, WV, 1988.

[2] Bonazza, T.J.; VanVoorhies, K.L.; Smith, J.E.: RF plasma ignition system concept for lean burn internal combustion engines, in *Proc. 27th Intersociety Energy Conversion Engineering Conf.*, San Diego, CA, 1992, 4.315–4.319.

[3] Stiles, R.D.; Thompson, G.J.; Smith, J.E.: Investigation of a radio frequency plasma ignitor for possible internal combustion engine use, in *SAE Paper 970071, SAE Int. Congress and Exposition*, Detroit, MI, 1997.

[4] McIntyre, D.L.: The coaxial cavity resonator as a prototype RF IC engine ignition source, Masters Thesis, West Virginia University, Morgantown, WV, 2000.

[5] Pertl, F.A.; Smith, J.E.: Feasibility of pulsed microwave plasma ignition for use in SI-engines, in *ICEF2007-1776, Proc. of the ASME Int. Combustion Engine Division 2007 Fall Technical Conf.*, Charleston, SC, 2007.

[6] Pertl, F.A.; Lowery, A.D.; Smith, J.E.: Investigation of wire grid modeling in NEC applied to determine resonant cavity quality factors. Appl. Comput. Electromagn. Soc. J., **22** (3) (2007), 420–423.

[7] Pertl, F.A.; Smith, J.E.: High-level modeling of an RF pulsed quarter wave coaxial resonator with potential use as an SI ignition source, in *SAE Paper SP-2180, SAE World Congress & Exhibition*, Detroit, MI, 2008.

[8] Wilhelm, J.P.; Pertl, F.A.; Wildfire, P.E.; Smith, J.E.: Ignition energy testing of the quarter wave coaxial cavity resonator with air-liquefied-gas mixtures, in *AIAA Paper 2008-3775, 39th American Institute of Aeronautics and Astronautics Plasmadynamics and Laser Conf.*, Seattle, WA, 2008.

[9] Van Voorhies, K.L.; Bonassa, T.L.; Smith, J.E.: Analysis of RF corona discharge plasma ignition, in *SAE Paper 929502, Technology for Energy Efficiency in the 21st Century, Proc. 27th Intersociety Energy Conversion Engineering Conf.*, San Diego, CA, 1992, 4.327–4.334.

[10] Lowery, A.L.; Pertl, F.A.; Smith, J.E.: Numerical investigation of the quarter wave coaxial cavity resonator quality factor through wire grid modeling in NEC, in *22nd Annual Review of Progress in Applied Computational Electromagnetics*, Miami, FL, 2006, 659–663.

[11] Lowery, A.D.: An experimental and computational investigation of dielectrics for use in quarter wave coaxial cavity resonators, Master Thesis, West Virginia University, Morgantown, WV, 2006.

[12] Pertl, F.A.; Smith, J.E.: Electromagnetic design of a novel microwave internal combustion engine ignition source, the quarter wave coaxial cavity igniter. Proc. Inst. Mech. Eng. D, J. Automob. Eng., **223** (11) (2009), 1405–1417.

[13] Gilmour, A.S.: Microwave Tubes, *Artech House* Inc., Norwood, MA, USA, 1986.

[14] Moreno, T.: Microwave Transmission Design Data. *Dover Publications*, New York, NY, 1948.

[15] Clayton, R.P.: Analysis of Multiconductor Transmission Lines. *John Wiley & Sons*, New York, NY, 1994.

[16] Pertl, Conical QWCCR Resonator Geometry, Plasma Internal Report 051102, West Virginia University/Center for Industrial Research Applications, Morgantown, WV, 1995.

**Franz A. Pertl** received his Bachelor of Science degrees in Electrical and Computer Engineering from West Virginia University (WVU), Morgantown, West Virginia, USA in 1994, and his Master of Science degree in Electrical Engineering from West Virginia University in 1996 and his Ph.D. in Mechanical Engineering from West Virginia University in 2008. He currently holds a program coordinator position with the mechanical and aerospace engineering department at West Virginia University and works as a Research Engineer for the Center of Industrial Research Applications (CIRA). He has also worked for the Engine and Emissions Research Center at West Virginia University and taught summer courses at the University. His areas of expertise include software design, data acquisition, microprocessor applications, color machine vision, controls, wind turbines and other areas of electrical engineering. He has published 26 conference papers, 8 journal papers and has been awarded 5 United States Patents to date and has been principal or co-principal investigator on several research projects. His current interests include electromagnetic and microwave plasma ignition. Dr. Pertl is a member of Sigma Xi Scientific Research Society and the Society of Automotive Engineers (SAE) International.

https://doi.org/10.1017/S1759078711000493 Published online by Cambridge University Press

**Mary Ann Clarke** assistant professor of mathematics at West Virginia University, is an applied mathematician with particular interests in scientific programming and engineering problem solving. Trained in materials engineering, classical mathematics, and numerical methods, she offers researchers in scientific disciplines a segue into physical modeling through the adaptation of empirical relationships and descriptive equations into computer codes. Winner of the 2010 WVU Foundation Award for Outstanding Teaching, she imparts to her students the utility of mathematics as an investigative tool as well as the importance of conceptual understanding and application of mathematical ideas to science and engineering.

**James E. Smith** received his Bachelor of Science and Master of Science degrees in Aerospace Engineering and Doctor of Philosophy degree in Mechanical Engineering from West Virginia University (WVU), Morgantown, West Virginia, USA in 1972, 1974, and 1984, respectively. He is currently the Director of the Center for Industrial Research Applications (CIRA) at West Virginia University, where he is also a Professor in the Mechanical and Aerospace Engineering (MAE) Department. He has taught at the University since 1976, before which he was a Research Engineer for the Department of Energy (DOE). During his 30-plus-year scientific career, he has been the principal and/or co-principal investigator for various projects funded by federal agencies (Tank-Automotive Armaments Command (TACOM), Department of Defense (DOD), HEW, Department of Transportation (DOT), US Navy, Defense Advanced Research Projects Agency (DARPA), and Department of Energy (DOE)), international corporations, and numerous US corporations. The work in these projects has resulted in the publication of 164 conference papers and 50 journal or bound transaction papers. This work has resulted in the granting of 31 United States Patents and numerous foreign patents on mechanical and energy-related devices. Dr. Smith is a member of American Institute of Aeronautics and Astronautics (AIAA), Society of Automotive Engineers (SAE) International, American Society of Mechanical Engineers (ASME), International Society for Computers and Applications (ISCA), American Society for Engineering Education (ASEE), and International Society for Instrumentation Engineers (SPIE).

https://doi.org/10.1017/S1759078711000493 Published online by Cambridge University Press